

PHYSICAL DESIGN OF BEAM TRANSPORT LINE OF A COMPACT TERAHERTZ FEL*

Han Zeng^{1,#}, Qushan Chen¹, Qiang Fu¹, Bin Qin¹, Bang Wu¹, Guangyao Feng², Yongqian Xiong¹,
Yuanjie Pei²

¹College of Electrical and Electronic Engineering, State Key Laboratory of Advanced Electromagnetic Engineering and Technology, Huazhong University of Science and Technology, Wuhan 430074, China

²NSRL, University of Science and Technology of China, Hefei 230029, China

Abstract

The single pass, linac-based compact terahertz source at HUST is now in the physical design stage. To match Twiss parameters and dispersion function of the electron beam at the undulator entrance and get smaller beta function in the whole line, several lattices based on the double bending achromat (DBA) structure were discussed and the optimized design is given with beam dynamics results—calculated by MAD and Trace 3D.

INTRODUCTION

The compact terahertz FEL device at HUST was initially designed to operate at 30-100 μ m (the energy of beam is 14-8 MeV, and the gap of the undulator is variable)[1,2]. The transport line applied in the device is to transport electron beam in the whole system efficiently and satisfy the requirements of characteristics parameters of the electron beam at the undulator entrance, and guarantees the achromaticity at the same time. Due to the space constraints, a simple structure with minimum number of components has been employed to achieve the targets.

In the first part, a basic requirements of the whole system and the layout of the transport line were presented; in the following section, the optics optimization and beam dynamics analysis are described.

BASIC REQUIREMENTS AND LAYOUT OF THE TRANSPORT LINE

The compact THz FEL is a normal conducting, 2.856 GHz linac driven FEL device. The required beam characteristics at the entrance of the undulator at 14MeV are shown in Table 1:

Table 1: Required Beam Characteristics at the Entrance of the Undulator

parameters	value	unit
α_H	1.0	
β_H	1.2	m
α_v	0.546	
β_v	0.246	m

The isochronicity and achromaticity of the transport line should be also guaranteed, and the linear beam transport optics may be reduced to a process of matrix

multiplication. At first order, the matrix equation is represented by

$$U_t = M_0^t U_0 \quad (1)$$

where $U = \{x, x', y, y', l, \Delta p/p_0\}^T$, and the elements in vector U are the phase-space coordinates of a particle, M_0^t is the transfer matrix[3,4,5]. Global achromaticity at the entrance of undulator is obtained when the transfer matrix elements R_{16} and R_{26} are both null thus making the transport line almost isochronous. Indeed, R_{51} , R_{52} and R_{56} are the governing isochronicity, and the isochronicity is obtained when these three matrix elements are null. R_{51} and R_{52} are linearly bound to R_{16} and R_{26} which means that when the latter are null the former are also null, and the required isochronicity is obtained [3,6]. After all, the space constraints should also be considered in the design.

The schematic layout of the whole system with a DBA structure is shown in Fig 1, the mirrors and waveguide were not shown.

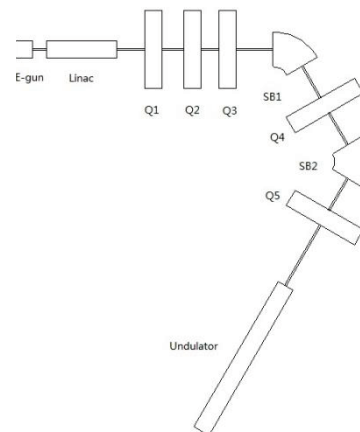


Figure 1: Schematic layout of the whole system.

The transport line locates between the linac and the undulator, and is consisted by quadrupole Q1, 2, 3, 4, 5 and two bending magnets (SB1, 2). The effective length of the quadrupole and bending magnets are 100mm and 200mm, respectively. The DBA structure is composed by SB1, SB2 and Q4. To minimize the length of the optical cavity, only one quadrupole, Q5 is located downstream of the DBA structure. And it also provides an adjustable variable of lattice close to the undulator entrance. The two uniform field bending magnets SB1 and SB2 deflect the beam by the same

angle 60°. To achieve a specific optical focusing property, the entrance and exit edge for these two bending magnets are paralleled [7].The quadrupole Q4 is configured at the centre of the DBA structure to make the transport line achromatic, and its field strength is independent from beam energy. The beam matching in the two transverse planes of the undulator is completed with the other four quadrupoles.

LATTICE DESIGN AND BEAM DYNAMICS

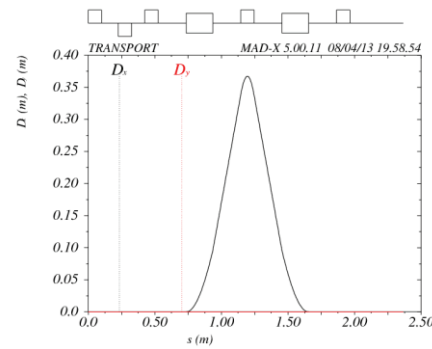
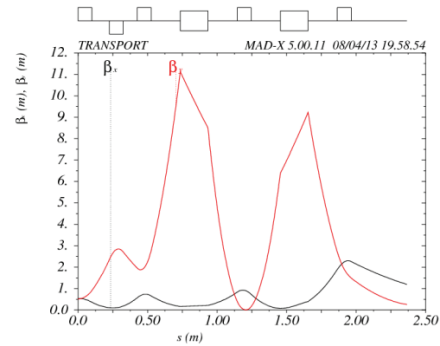
During the beam transport system optimization, two lattice design codes- MAD-X and TRACE-3D- were used to adjust the quadrupole field strength at first order to satisfy the requirements of the characteristics of the electron beam at the entrance of the undulator.

Table 2: The Parameters of the Beam at the Entrance of The Transport Line

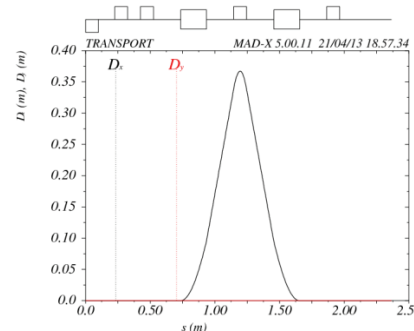
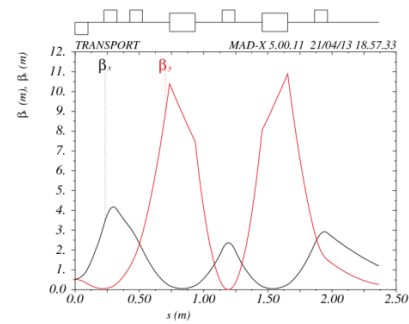
parameters	value	unit
energy	14.48	Mev
α_H	-0.285	
β_H	0.535	m
α_v	-0.2713	
β_v	0.514	m
Horizontal Normalized Emittance(RMS)	6.667	Pi-mm-mrad
Vertical Normalized Emittance(RMS)	6.603	Pi-mm-mrad
σ_H	0.35	mm
σ_v	0.34	mm
Charge	200	pc

The procedure of optimization is divided into two steps: (1) the field strength parameters of Q4 is fitted to make the dispersion function null at the end of DBA structure, thus making the transport line almost isochronous; (2) the field strength parameters of Q4 fitted in the first step is fixed, then Q1, Q2, Q3 and Q5 were fitted to make the waists of beta function at the centre of undulator in both horizontal and vertical plane. The condition of angle dispersion functions at the exit of the DBA structure is ignored, since there are not enough degrees of freedom to satisfy all the targets. The required beam characteristics at the entrance of the undulator is shown in Table1. In the undulator, the beta functions in the two planes are symmetric with respect to the centre of the undulator. Table 2 shows the parameters of the beam at the entrance of the transport line at 14Mev, and the axial beam parameters were obtained as rms bunch length $\sigma_t=10ps$ and rms energy spread $\Delta E/E=0.13\%$. And the hard edge models without fringe field of the quadrupoles and sector bending magnets were introduced to the optimization of the lattice. Fig.2 illustrates the beta and dispersion functions in the

transport line of two lattices, and the focusing strength of the quadrupoles are shown in Table 3. Both these two lattices satisfied the requirements of the characteristics of the electron beam at the entrance of the undulator. And the elements in the globe transfer matrixes are shown in Table 4.



(a) Lattice1



(b) Lattice 2

Figure 2: The beta and the dispersion function of (a) lattice 1 and (b) lattice 2.

Table 3: The Focusing Strength of the Quadrupoles

Quadrupoles	Lattice 1	Lattice 2	Unit
Q1	49.8566	-66.3165	m^{-2}
Q2	-43.3292	43.1341	m^{-2}
Q3	71.8402	14.9990	m^{-2}
Q4	64.6102	64.6102	m^{-2}
Q5	32.1723	39.1378	m^{-2}

Table 4: The Elements in the Globe Transfer Matrixes

Elements	Lattice 1	Lattice 2
R_{16}	-7E-6	-5.91E-9
R_{26}	4.2E-5	5.8E-5
R_{51}	3E-6	8.6E-5
R_{52}	2.8E-5	2E-6
R_{56}	-0.0664	-0.0664

It is indicated that in these two lattices, global achromaticity at the entrance of undulator is obtained since the transfer matrix elements R_{16} , R_{26} , R_{51} and R_{52} are both almost null, and the transport line is a nearly isochronous system since $R_{56} = -0.0664m$, and the final scheme is still not determined since the performance of the lattices are basically the same. At present, the lattices design is based on the hard edge model, further simulations with realistic magnetic fields will be considered to decide which one to employ.

The envelopes of the beams are presented in Fig 3. The maximum value of envelop is about 1.7mm, which occurs in the DBA structure.

DISCUSSION AND CONCLUSIONS

In the paper, the layout of the transport line was presented, and also the lattice designs and beam dynamic analysis. The two lattices presented in the paper both satisfy the requirements of the characteristics of the electron beam at the entrance of the undulator. The result indicated that global achromaticity at the undulator entrance is obtained since the transfer matrix elements R_{16} , R_{26} , R_{51} and R_{52} are both almost null, and the transport line is a nearly isochronous system since $R_{56} = -0.0664m$. The original design is based on the hard edge model, further simulations with realistic magnetic fields will be considered.

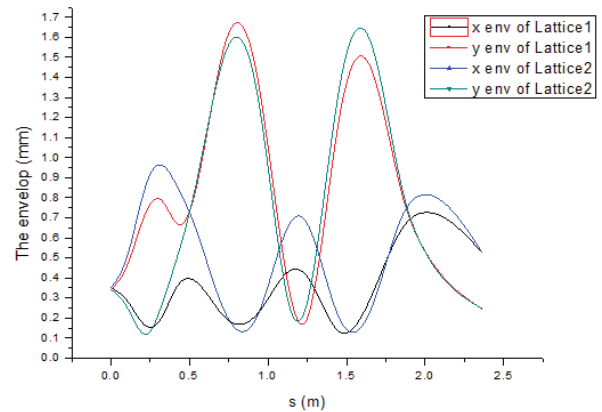


Figure 3: The envelope of the beams with different lattices.

REFERENCES

- [1] XIONG Yong-Qian, QIN Bin et al., Preliminary Design of Compact FEL Terahertz Radiation Source (in Chinese), Chinese Physics C, Vol32, supplement I, Mar, 2008.
- [2] TAN Ping, HUANG Jiang et al., Terahertz radiation sources based on free electron lasers and their applications, SCIENCE CHINA, January 2012 Vol. 55, No. 1: 1–15.
- [3] C. Rippon, Study and optimization of the electron beam transport line of the FEL CLIO, Nuclear Instruments and Methods in Physics Research A 445 (2000) 399-403.
- [4] K.R. Crandall, D.P. Rusthoi, Trace3-D Documentation, 3rd Edition, Los Alamos National Laboratory, May 1997.
- [5] K.L. Brown et al., Transport, a computer program for designing charged particle beam transport systems, CERN 80-04.
- [6] Ryoichi Hajima, Masaru Sawamura et al., Design of energy-recovery transport for the JAERI FEL driven by a superconducting linac, Nuclear Instruments and Methods in Physics Research A 445 (2000) 384-388
- [7] European Organization for Nuclear Research, User's Guide of MAD-X, <http://madx.web.cern.ch/madx/>